AD-759 509

MODELING OF CO/N_2 MOLECULAR LASER SYSTEMS

Edward R. Fisher, et al

Wayne State University

Prepared for:

Army Research Office-Durham

6 February 1973

MODELING OF CO/N_2 MOLECULAR LASER SYSTEMS

SEMI-ANNUAL TECHNICAL REPORT

EDWARD R. FISHER, ALLAN LIGHTMAN, RICHARD MARRIOTT

FEBRUARY 6, 1973

U. S. ARMY RESEARCH OFFICE - DURHAM

DA-ARO-D-31-124-72-G 103

WAYNE STATE UNIVERSITY
RESEARCH INSTITUTE FOR ENGINEERING SCIENCES
DETROIT, MICHIGAN 48202

APPROVED FOR PUBLIC RELEASE;
DISTRIBUTION UNLIMITED.

The views and conclusions contained in this document are those of the authors and should not be interpreted as necessarily representing the official policies, either expressed or implied, of the Advanced Research Projects Agency or the U. S. Government.

33 R

Security Classification

DOCUMENT CONTROL DATA - R & D

(Security classification of title, body of abstract and indexing annotation must be entered when the overall report is classified)

1. ORIGINATING ACTIVITY *(Corporate author)*

Wayne State University
Research Institute For Engineering Sciences
Detroit, Mich. 48202

2a. REPORT SECURITY CLASSIFICATION

UNCLASSIFIED

2b. GROUP

NA

3. REPORT TITLE

Modeling of CO/N_2 Molecular Laser Systems

4. DESCRIPTIVE NOTES *(Type of report and inclusive dates)*

Semi-Annual Technical Report; June 30, 1970 to January 25, 1973

5. AUTHOR(S) *(First name, middle initial, last name)*

Edward R. Fisher, Allan Lightman, Richard Marriott

6. REPORT DATE

February 6, 1973

7a. TOTAL NO. OF PAGES

28

7b. NO. OF REFS

20

8a. CONTRACT OR GRANT NO.

DA-ARO-D-31-124-72-G 103

b. PROJECT NO.

62301-D

c.

ARPA Order No. 675 AMDT 11

d.

9a. ORIGINATOR'S REPORT NUMBER(S)

None

9b. OTHER REPORT NO(S) *(Any other numbers that may be assigned this report)*

----

10. DISTRIBUTION STATEMENT

Approved For Public Release; Distribution Unlimited

11. SUPPLEMENTARY NOTES

----

12. SPONSORING MILITARY ACTIVITY

U.S. Army Research Office - Durham
Box CM, Duke Station
Durham, N. Carolina 27706

13. ABSTRACT

Over the past three years an extensive molecular laser modeling code has been developed under ARPA sponsorship. This model characterizes the time evolution of pulsed molecular laser systems including the effects of non-Boltzmann electron distributions, stimulated emission processes, temperature and density transients and state-of-the-art energy transfer rate coefficients. During the last year a laboratory effort has been developed to complement these analytic studies. This report ~~will~~ describe the results obtained from the modeling studies and the current status of the laboratory effort.

7

DD FORM 1 NOV 65 1473 REPLACES DD FORM 1473, 1 JAN 64, WHICH IS OBSOLETE FOR ARMY USE.

Security Classification

Abstract

Over the past three years an extensive molecular laser modeling code has been developed under ARPA sponsorship. This model characterizes the time evolution of pulsed molecular laser systems including the effects of non-Boltzmann electron distributions, stimulated emission processes, temperature and density transients and state-of-the-art energy transfer rate coefficients. During the last year a laboratory effort has been developed to complement these analytic studies. This report will describe the results obtained from the modeling studies and the current status of the laboratory effort.

Introduction

Over the past three years an extensive molecular laser modeling code has been developed at Wayne State University under ARPA sponsorship.(1,2) Early applications of this dynamic model were made to small signal gain measurements in a TEA pulsed CO laser system.(3) The agreement (1) obtained suggested the application of the laser code to new CO laser systems in an attempt to provide a guide to experimentation in optimizing the gain particularly on the low lying CO transitions.(2) The results of this application are in agreement with recent measurements in which substantial gain was found in a low temperature pulsed N_2/CO laser system.(4)

Laboratory experiments aimed at detailed measurements of small signal gain and CO laser output are currently underway and an extension of our laboratory effort to produce gain profiles and laser intensity versus wavelength data for use in further understanding laser phenomenology is in progress.

The quantum mechanical close coupling code has been extensively applied over the past few years to calculations of the vibrational transitional (VT) excitation cross sections for the species CO_2,H_2O,H_2,CO,N_2 and He.(5) During the last year, this close coupling code has been extended to calculate vibration-vibration (VV) cross sections for an arbitrary collision pair for which general information is available in the interaction potential. Currently this code is being applied to CO-CO VV cross sections due to the availability of experimental data.(6,7)

In the remaining sections of this report, the current results from the molecular laser code are outlined, experimental data pertinent to our current laser program presented and a brief presentation of preliminary close coupling VV cross sections are given.

II. Molecular Laser Modeling Code

The molecular laser model developed under the ARPA/ARO-D sponsored research program characterizes the time evolution of the separate vibrational levels of a multicomponent mixture of two molecular species and inert diluents in the presence of hot electrons of arbitrary density, pulse shape and pulse duration. Included in this formulation are multi-quantum electron-molecule energy transfer processes, single quantum VV and VT processes and spontaneous and stimulated emission processes. The system of coupled rate equations obtained from these processes has been typically applied to a system of from 20 to 30 vibrational levels in each of two diatomic species. The time integration of the resulting system of coupled nonlinear differential equations is performed using a Runge-Kutta-Merson procedure with an algebraic subroutine to handle "stiffness". An extensive discussion of the basic components in this molecular laser model as applied to CO laser systems has been described extensively in the literature (1,2) and can be referenced in Appendices I and II. In the following we outline the recent developments in the laser code.

Non-equilibrium Plasma Code

It has been clear for some time that non-Boltzmann electron energy distribution functions generally exist in molecular laser systems. (8) Particularly as interest in focused on visible and UV excitation in molecular systems, a knowledge of the exact form of the electron energy distribution becomes critical to estimates of excitation rates. In addition, the interesting effects of gas additives on laser gain and wavelength in CO suggests that the plasma properties are being altered rather than a direct effect via molecular energy transfer processes. (9) Since a shift in available laser wavelength toward higher energy photons (lower vibrational transitions) has been noted, particular interest is viewed toward plasma predictions in multicomponent infrared laser systems.

In order to calculate the electron energy distribution in the CO laser we must solve the following form of the Boltzmann equation for the distribution function f(u):$^{(10)}$

$$(1)\quad \frac{E^2}{3}\,\frac{u}{NQ_m}\,\frac{df}{du} + \frac{2m}{M}\left[u^2NQ_m f + \frac{kT}{e}\,u^2NQ_m\,\frac{df}{du}\right] = -N\sum_j\left\{\int_0^{u_j} du_j'(u'+u)Q_j(u'+u)\,f(u'+u) - \int_0^{u_j} du'(u'-u)Q_j(u'-u)\,f(u'-u)\right\}$$

where u = electron energy

u_j = threshold energy for the j^{th} vibrational or electron molecular energy level

m = electron mass

M = molecular mass

N = molecular density

E = electric field

Q_m = momentum transfer cross section for electron-molecule collisions

$Q_{\pm j}$ = cross section for electron impact excitation or deexcitation of the j^{th} molecular vibrational or electronic state

T = gas temperature

The above form of the Boltzmann equation involves the following assumptions:

1) a uniform weak de-electric field
2) steady state
3) low density of ions, electrons, and excited molecules

4) large elastic cross section compared to inelastic cross section
5) mean free path small compared to the dimensions of the laser tube
6) the proportion of ionizing to exciting collisions is negligible.

If in the form of the Boltzmann equation above, we make the following dimensionless substitutions:

$$z = \frac{eu}{kT}, \quad \alpha = \frac{M}{6M}\left(\frac{eE}{NQ_0 kT}\right)^2, \quad \theta = \frac{Q_m}{\alpha_0}, \quad \eta_{\pm j} = \frac{M}{2m}\frac{Q_{\pm j}}{Q_0}$$

(where Q_o is some arbitrary constant chosen to make the numbers θ and η more manageable, we used $Q_o = 10^{-16}$ cm^2) we obtain

$$\theta z(z + \alpha/\theta^2)\frac{df}{dz} + \theta z^2 f = -\sum_j \left\{\int_0^{z_j} d\xi(\xi+z)\eta_j(\xi+z)f(\xi+z) - \int_0^{z_j} d\xi(z-\xi)\eta_{-j}(z-\xi)f(z-\xi)\right\} \tag{2}$$

If, neglecting the second (superelastic) integral, we let

$$g = \sum_j \int_0^{z_j} d\xi(\xi+z)\eta_j(\xi+z)f(\xi+z) \tag{3}$$

and then differentiate this with respect to z we obtain

$$\frac{dg}{dz} = \sum \left[(z+z_j)\eta_j(z+z_j)f(z+z_j) - z\eta_j(z)f(z)\right] \tag{4}$$

Substituting (3) into (2) we obtain

$$(5)\quad \frac{df}{dz} = -\frac{1}{z+\alpha/\theta^{2}}\left[zf(z) + g(z)/\theta z\right]$$

Equations (4) and (5) are simultaneous first order differential equations for the distribution function and the inelastic collision integral. We solve these numerically using a fourth order Runge-Kutta integration scheme. Since f(z) is strictly monotonically decreasing with increasing energy z and $f(\infty)=0$ we start our integration at large z where f(z) is small and integrate in toward zero. That is, the distribution function is of the form,

$$\begin{aligned}(6)\qquad f(z) &= \int_0^z K(z')\,dz' \\ &= \int_0^\infty K(z')\,dz' - \int_z^\infty K(z')\,dz' \\ &= \cancelto{0}{f(\infty)} + \int_\infty^z K(z')\,dz' \\ &= \int_\infty^z K(z')\,dz'\end{aligned}$$

Of course, instead of starting the integration at infinity we start at a large but finite z chosen such that the truncation error is negligible. In this way we are able to deal with the non-locality of the Boltzmann equation.

The initial values for f(z) and g(z) are obtained using an approximate solution to the Boltzmann equation given by Holstein.(11) This solution is found assuming the following,

1) the super-elastic integral can be ignored

2) the term $\frac{kT}{e} u^2 NQ_m \frac{df}{du}$ which accounts for molecular motion can be ignored

3) the momentum transfer cross section is constant with energy

4) the total excitation cross section is a step function: o for $u < u_e$ and constant for $u > u_e$

a solution to the Boltzmann equation is,

$$(7) \qquad f_H(u) = \left(\frac{u_e}{u}\right)^{\frac{1}{2}} e^{-\gamma\left(\frac{u}{u_e} - 1\right)}$$

where $\gamma = \left(2 \frac{u_e}{e} \frac{Q_m}{E/N}\right)\left(\frac{3}{2} Q_e/Q_m\right)^{\frac{1}{2}}$

u_e = the threshold energy for excitation
Q_e = the total excitation cross section
Q_m = the momentum transfer cross section.

The conditions for the validity of this approximation are,

$$u \geq u_e \ , \quad \gamma >> 1 \ , \quad \frac{2m}{M} \ \frac{\gamma^2}{Q_e/Q_m} << 1$$

Note that $f_H(u_e) = 1$. That is, this solution is unnormalized. To make this approximation a little more realistic we assume that f(u) in the energy range $u \leq u_e$ is given by the solution to the Boltzmann equation with the inelastic integral equal to zero. This solution (properly normalized) is Dryvestyn and is

$$(8) \quad f_D(u) = \frac{2^{\frac{1}{4}}}{\Gamma(\frac{3}{4})} \left[\frac{M}{6m} \ \frac{1}{Q_m^2} \ \left(\frac{E}{N}\right)^2\right]^{-\frac{3}{4}} e^{-\frac{u^2 Q_m^2}{M/3m(E/N)^2}} \qquad (u \leq u_e)$$

We now use $f(u) = f_D(u_e) * f_H(u)$, $(u \geq u_e)$ to calculate the initial values for the Runge-Kutta integration sequence. This technique gives good starting values but, as it turns out, the final result for f(z) after normalization is only weakly dependent upon the starting values of the integration provided the integration is started at large enough z.

Some typical results for the electron energy distribution function using the above approach are shown in Figure 1. The conditions for this calculation in pure CO are the same as stated by Nighan(8) for comparison. Nighan's results are replotted in Figure 1a. Although qualitatively similar, the E/N values for the comparative calculations are displaced by one curve. The source of this discrepancy is under review. Clearly, the distributions are highly non-Boltzmann and their presence will strongly affect calculations involving excitation energies above about 2 or 3 ev, depending on the E/N value. The sensitivity to input cross section values is shown in Figure 2 where the electronic cross sections are arbitrarily reduced by a factor of 10 (curve A) and the vibrational excitation cross sections reduced by 2 (curve B) over the nominal values. The effect of superelastic collisions in CO on the form of the electron energy distribution is shown in Figure 3 for two CO vibrational temperatures using the nominal cross section values of Figure 1.

The running time for the above calculations is approximately 1 min CPU on an IBM 360/67 system, indicating that the method is not only stable but very fast. Since the run time for the generation of the electron distribution function is so rapid, it becomes feasible to perform a fully coupled electron distribution calculation with a time evolving vibrational distribution appropriate to a pulsed laser system. Calculations are currently underway to predict the form of the distribution function in the case of CO laser mixtures.

Figure 1: Calculated electron distribution functions for a pure CO laser system using the conditions of Nighan(17).

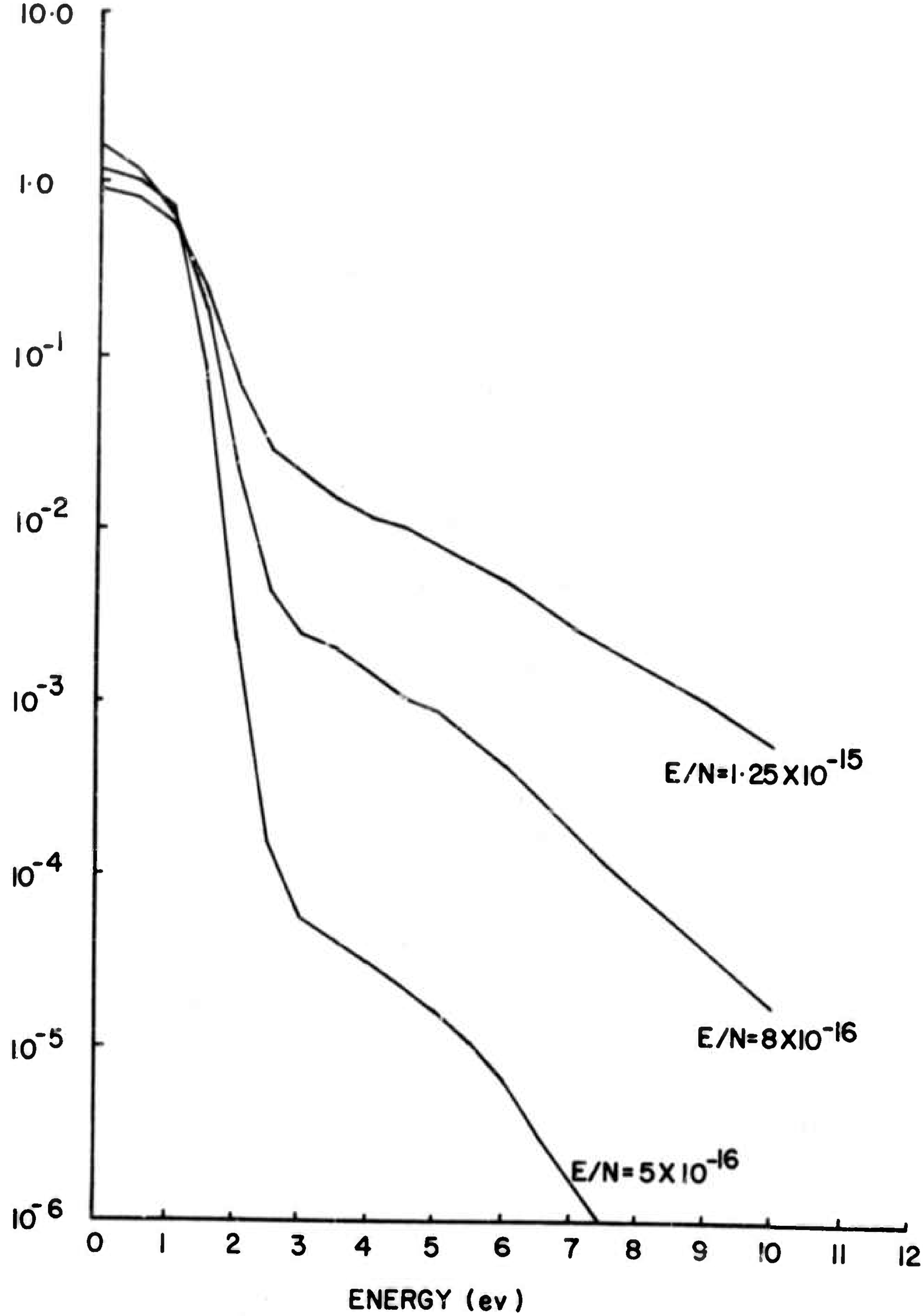

Figure 1a: Calculated electron distribution functions from the publication of Nighan(17) for comparison to Figure 1.

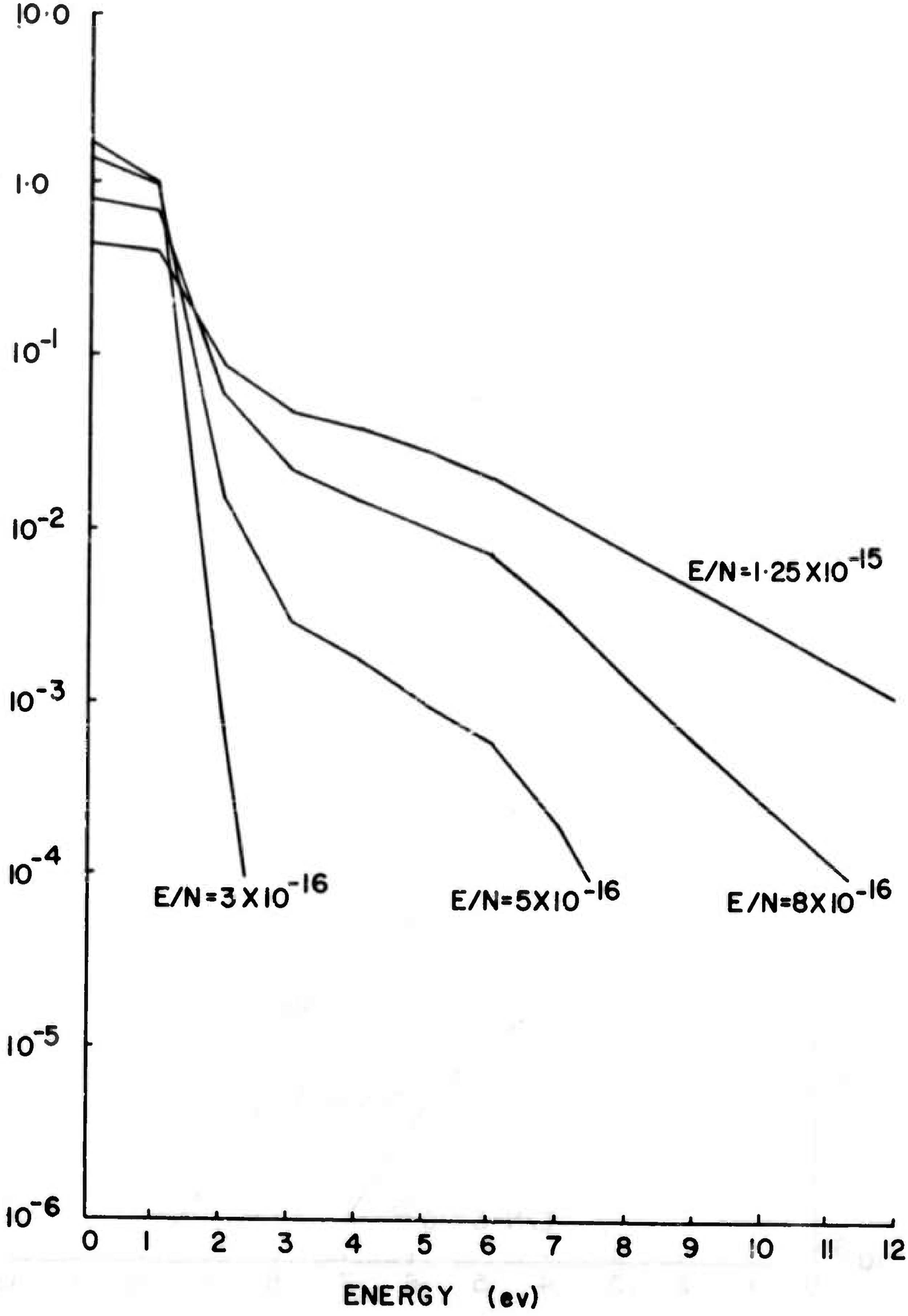

Figure 2: Variation in calculated electron distribution functions with arbitrary changes in the input cross section values for a given value of E/N.

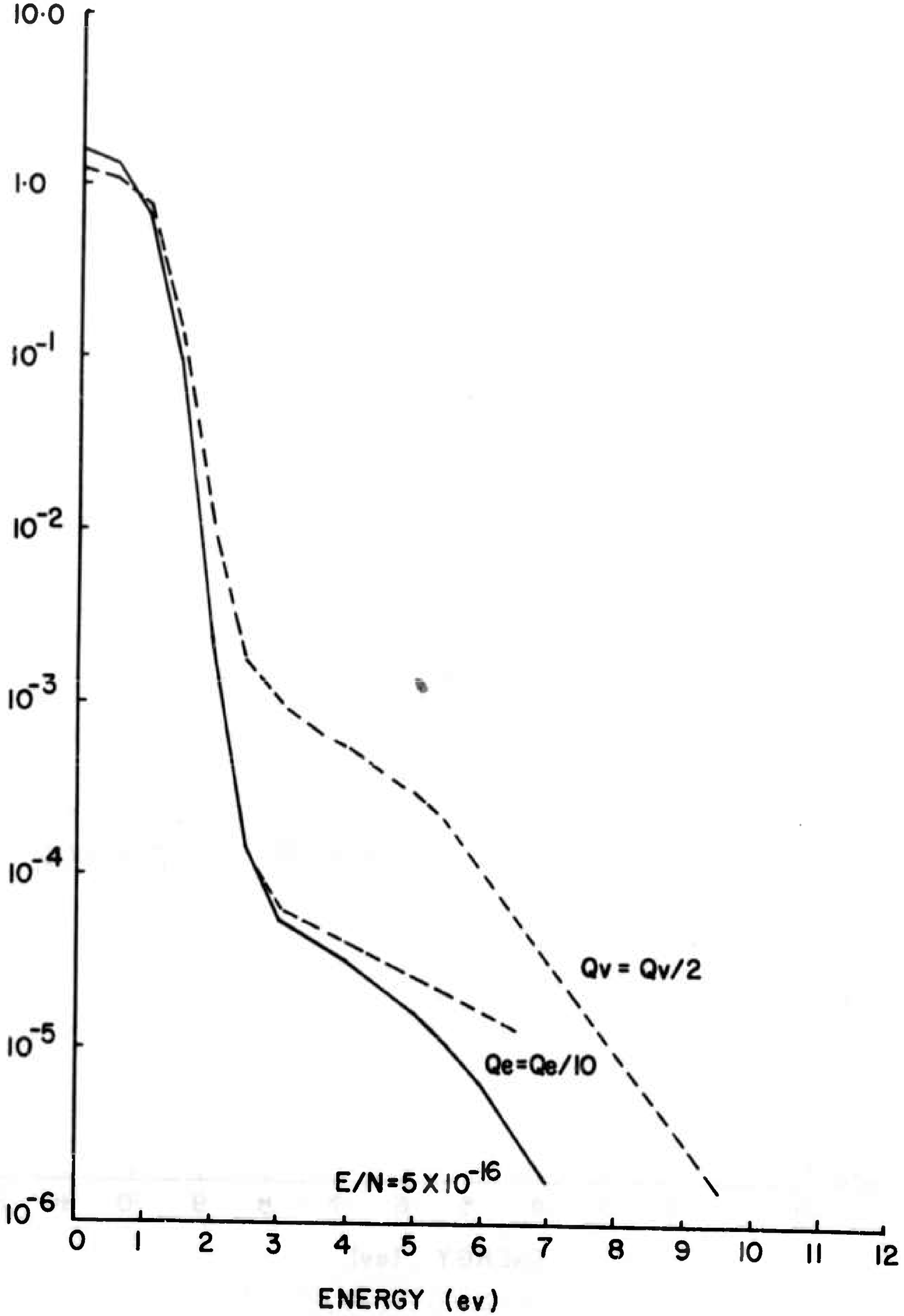

Figure 3: Variation in calculated electron energy distribution functions for different CO vibrational temperatures at an E/N of 5 X 10^{-16}.

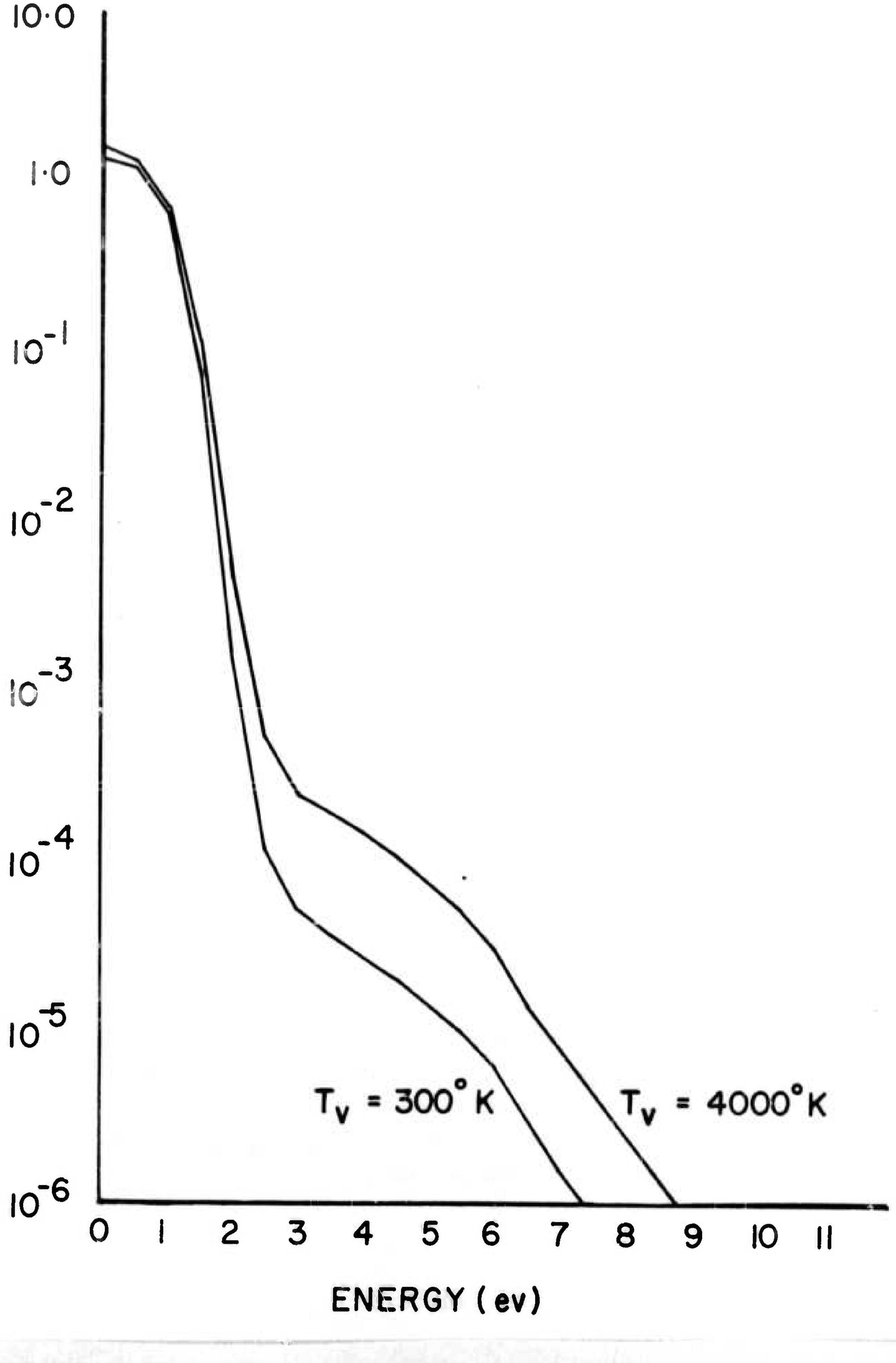

Energy Transfer Rate Coefficients

Past applications of the molecular laser code have used VV rate coefficients based upon the short range force model of Rapp and Englander-Golden(12) modified to fit the experimental data of Hancock and Smith.(6,7) Since this method is not at all reliable for the estimate of the temperature dependence of VV rates for near resonant processes, we have added to the laser code the long range force model developed by Sharma(13) and outlined by Jeffers and Kelley.(14) The basis for this long range force model has been extensively discussed in the literature.(14) Figure 4 shows the present VV coefficients for CO at 300°K as compared to the available measurements.(6) We are currently completing the quadrupole-quadrupole interaction case to generate N_2-N_2 near resonant VV rate coefficients. These will be inserted into the code for future laser model predictions.

Stimulated Emission Processes

Past published results on the application of the laser code has not explicitely included stimulated emission processes in the prediction of the time sequence of small signal gain available from a pulsed CO laser.(1,2) In order to demonstrate this current capability, we performed a calculation on the room temperature TEA CO pulsed laser used by Jeffers(3) in which the 6-5 J=26 (upper state) transition was stimulated and subsequent small signal gain calculated, Figures 5 and 6 show the maximum gain profiles for a particular vibrational transition without and with stimulated emission processes, respectively. The power output in the 6-5 J=26 transition is calculated to be 1996 watts with a pulse width (width at half maximum) of .23μ second. A similar calculation for 7-6 J=26 stimulated is shown in Figure 7. The power output for this case is 1047 watts with a pulse width of .25μ seconds.

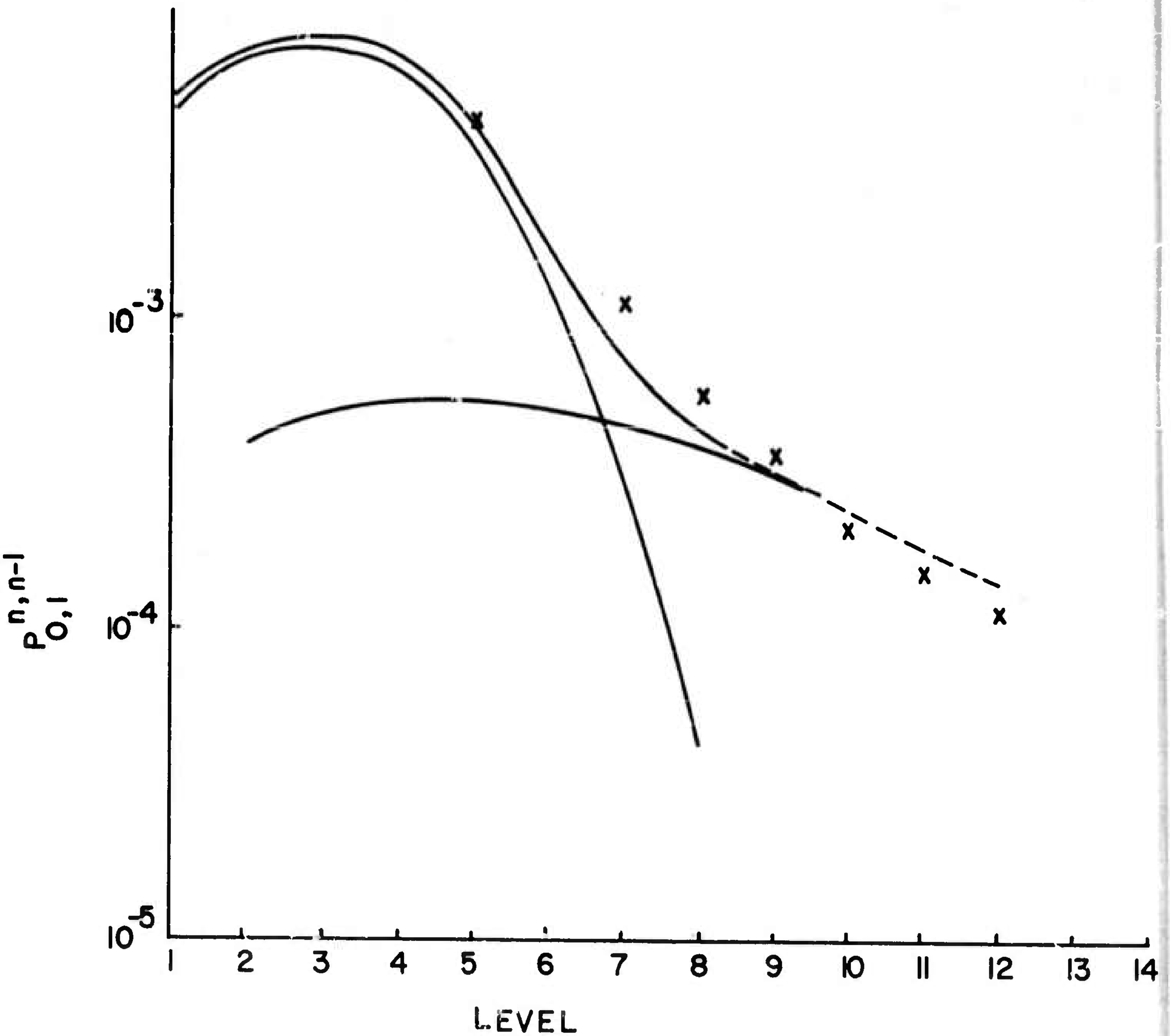

Figure 4: Calculated VV exchange rate coefficients including both short range and long range contributions. The data points are from Hancock and Smith(15) for pure CO-CO collisions.

Figure 5: Small signal gain predictions for a pulsed CO laser with a pulse width of 0.6 sec. The CO pressure is approximately 30 torr using the conditions of Jeffer and Wiswall(3)-also see Appendix I.

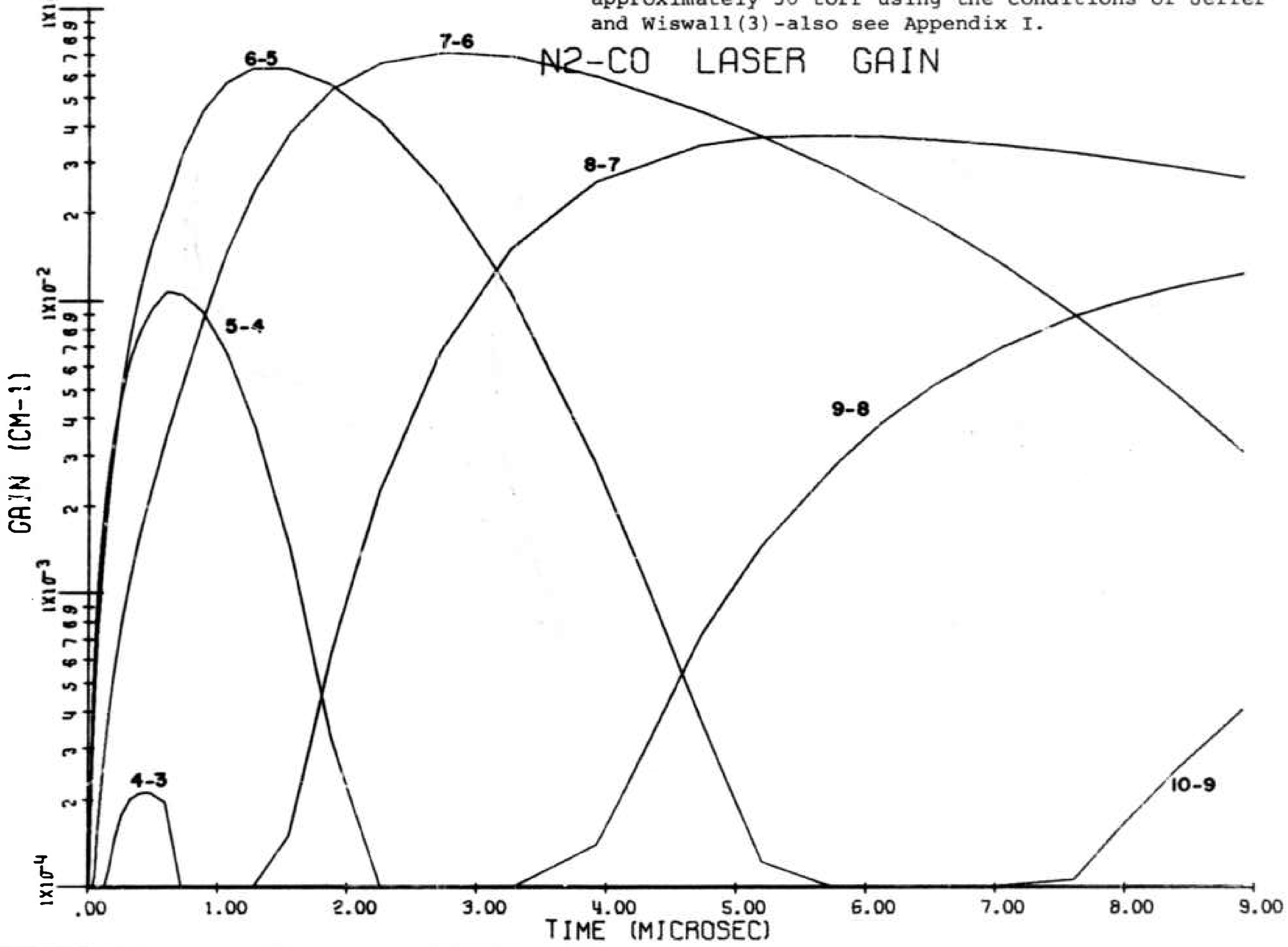

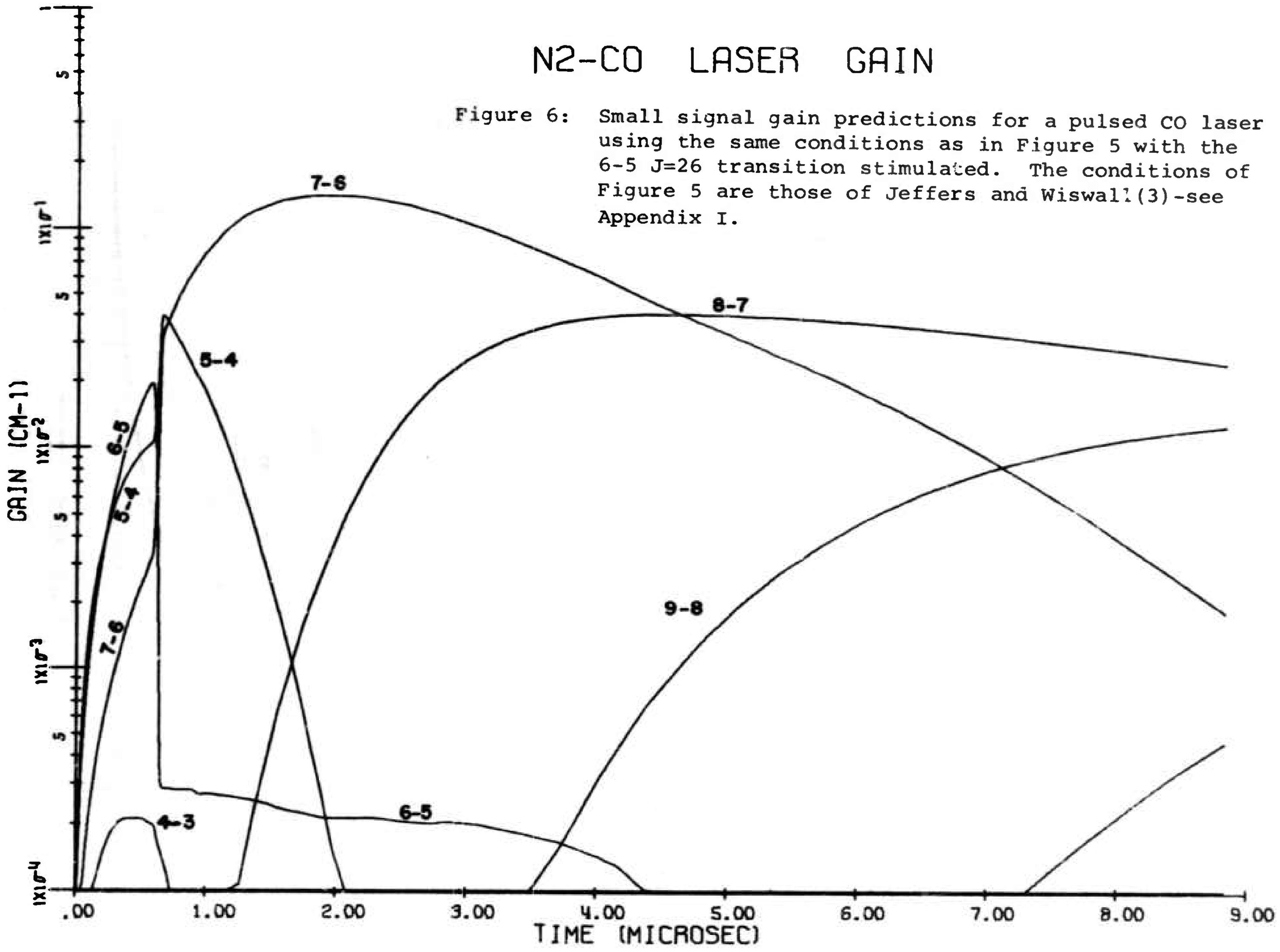

Figure 6: Small signal gain predictions for a pulsed CO laser using the same conditions as in Figure 5 with the 6-5 J=26 transition stimulated. The conditions of Figure 5 are those of Jeffers and Wiswall(3)-see Appendix I.

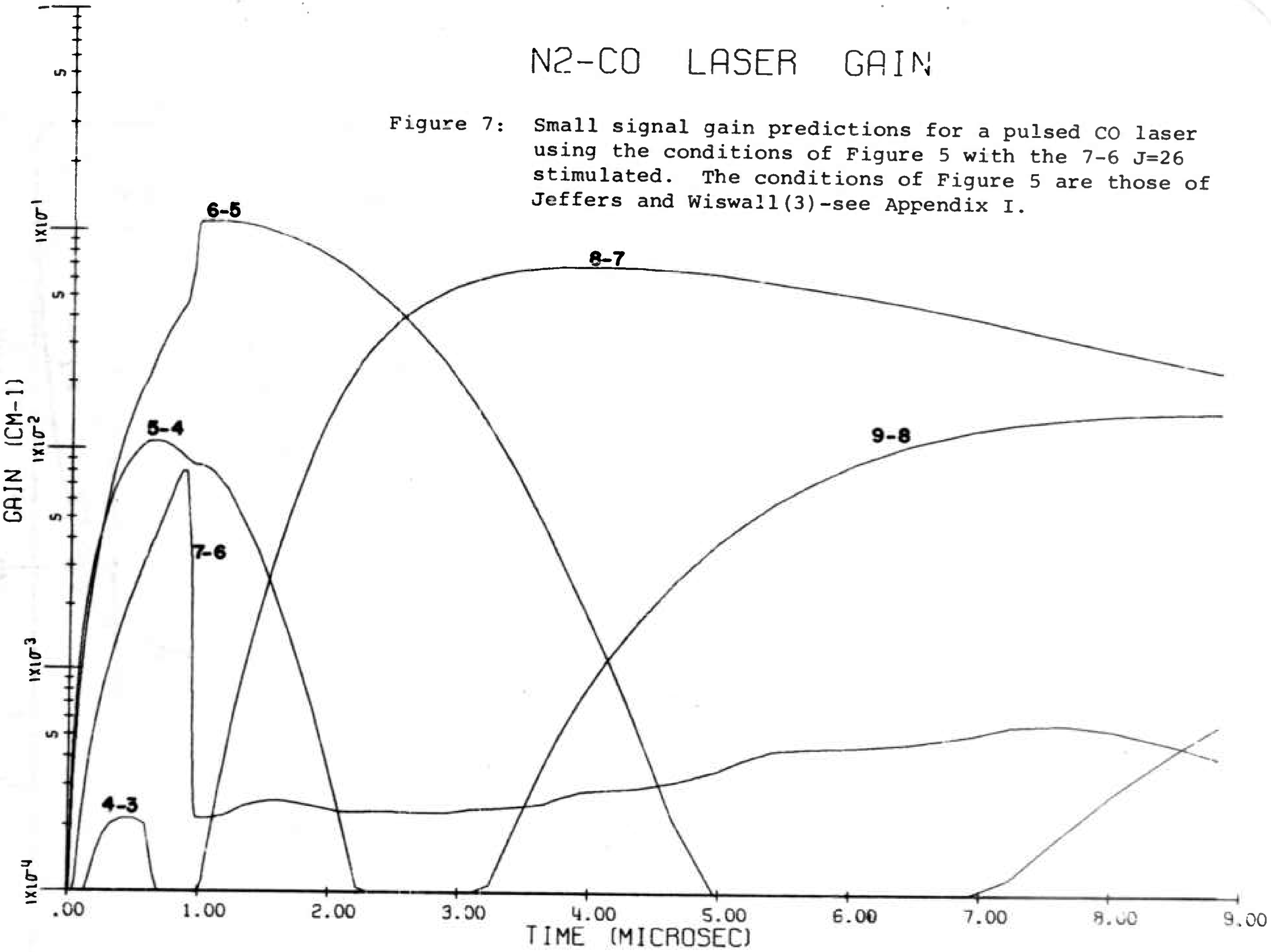

Figure 7: Small signal gain predictions for a pulsed CO laser using the conditions of Figure 5 with the 7-6 J=26 stimulated. The conditions of Figure 5 are those of Jeffers and Wiswall(3)-see Appendix I.

As can be clearly seen, the gain on both the 7-6 and the 5-4 transitions are enhanced due to depopulating the lower state and populating the upper state, respectively. Subsequent stimulation of the 5-4 transition at the optimum time delay would produce enhance 5-4 power output over that of the unstimulated case. The possibility of stimulating the 3-2 transition in the LN_2 cooled N_2/CO laser(2) followed by stimulating the 2-1 transition could produce substantial power output in this high photon energy range. Calculations using this stimulated emission capability are being performed in an attempt to further optimize available power output on low level transitions.

Sidelight Infrared Spectra

The spontaneous emission sidelight spectra code is fully operational either using a predefined vibrational distribution (i.e. Treanor type(15)) or the direct output of the calculated vibrational distribution from the laser code. The harmonic or first overtime spectra can be generated as a line by line calculation integrated over an arbitrary slit function. An example of the predicted sidelight first overtone spectra is shown in Figure 8 for a Treanor distribution having $\theta_1^* = 2700^\circ K$ and a rotational temperature of 375° (the slit function is assumed to be triangular with a width at half height of 6.6 mμ. A roughly equivalent experimental spontaneous emission spectra obtained from a CW N_2/CO laser system in the laser laboratory is shown in a later section of this proposal.

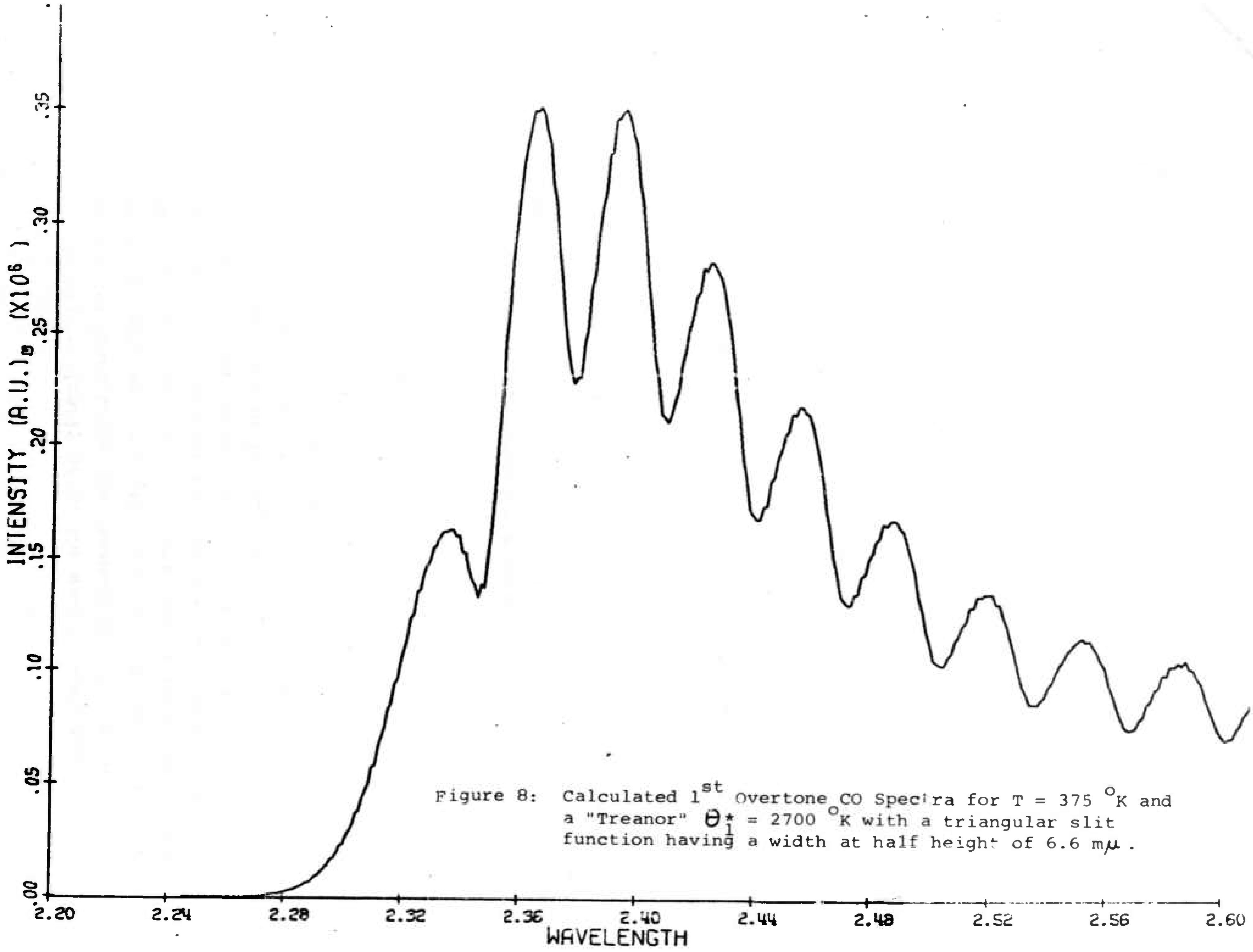

Figure 8: Calculated 1st Overtone CO Spectra for $T = 375\ ^{o}K$ and a "Treanor" $\Theta_1^* = 2700\ ^{o}K$ with a triangular slit function having a width at half height of 6.6 mμ .

III. Theoretical Determination of VV and VT Rate Coefficients

Modeling of molecular gas laser systems requires a knowledge of the reaction rates for a wide range of excitation and de-excitation collision processes under a wide range of gas kinetic conditions. At best this data is difficult to obtain either experimentally or theoretically, and a combination of approaches is necessary to estimate values for the parameters involved.

The theoretical program at RIES has been primarily concerned with the calculation of cross sections for the vibrational excitation of molecules by heavy body collisions. This is carried out using a numerical close coupling solution of the wave equation for the colliding system based on the breathing sphere model of Schwartz, Slawsky, and Herzfeld (16) to represent the target molecular vibrator and an empirical spherically symmetric scattering potential, but neglecting any structure in the impacting particle.

To this approximation a variety of collision systems have been studied (CO^*-CO; CO^*-O(^1D); CO_2^* - CO_2; CO_2^*-N_2; CO_2^* - H_2; CO_2^* - H_2O; H_2O^* - H_2O; H_2O^* - H_2; and H_2O^* - CO_2 where * indicates the target vibrator). Many of the results and references are collected in the recent report by Fisher (5) . However, these studies were limited to the case of vibrational - translational (VT) energy transfer processes. For many gas mixtures of interest (eg. CO - N_2) direct vibration - vibration (VV) energy transfer processes are also important. Nevertheless no calculations of such processes to the precision afforded by the close coupling approximation have been published up to the present time.

The RIES molecular collision code has now been extended to include vibrational states in the impacting particle. This in turn permits both the calculation of significant VV cross sections simultaneously with the VT cross sections, within the same breathing sphere approximation and the estimation of the effect produced on target particle VT cross sections by coupling in the impact particle states.

Calculations on the CO - CO system are currently underway to debug the revised code, to study the magnitude of VV cross sections for states in exact energy resonance and to determine the effect of the impact particle states on the calculated VT cross section for the excitation of the first vibrational level of CO from the ground state. This cross section dominates the vibrational relaxation of CO and the previous VT results were in good agreement with experiment. Consequently, for this system, the VT cross section should not be particularly sensitive to the addition of impact particle states.

Preliminary results are shown in Table I. Conclusions drawn from these values must be speculative since the total cross sections, which are the physically important quantities, involve summation over approximately 100 partial waves rather than the single partial cross section shown. Nevertheless, it is interesting to note that the partial cross section dominating the process of vibrational relaxation has been little changed (30% decrease) from the original VT result although the VV cross sections themselves are large and indicate that exchange processes such as

$$\mathrm{CO}(0) + \mathrm{CO}(2) \longrightarrow \mathrm{CO}(1) + \mathrm{CO}(1)$$

are orders of magnitude faster in the depopulation of the higher vibrational levels than the VT process

$$CO(0) + CO(2) \longrightarrow CO(1) + (.266\ ev)\ .$$

At the present time these CO calculations are being extended over all significant partial waves, the number of coupled states required for convergence of the cross sections is being investigated and it is intended to study the sensitivity of the VV cross sections to the form of the long range scattering potential. Finally, the theoretical results will be compared with the available experimental values (6,7) and a report issued in the near future.

Table I Calculated cross sections for the vibrational excitation of CO by head-on collisions (zero order partial wave) with CO. (in units of πa_o^2).

	Collision process				Zero order partial cross section		
	A(i)+B(n)	→	A(j)+B(m)		Coupling retained: A states (0) B states (0,1,2)	A states (0,1) B states (0,1,2)	
	CO(0)+CO(0)+1eV	→	CO(0)+CO(0)+1eV	†	1.78(-3)	1.29(-3)*	
**	CO(0)+CO(0)+1eV	→	CO(0)+CO(1)+.734eV		6.32(-8)	3.92(-8)	**
		→	CO(1)+CO(0)+.734eV		———	1.63(-8)	
	CO(0)+CO(0)+1eV	→	CO(0)+CO(2)+.468eV		1.63(-13)	8.34(-14)	
	CO(1)+CO(1)+.734eV	→	CO(1)+CO(1)+.734eV		3.93(-4)	1.16(-4)	
	CO(1)+CO(1)+.734eV	→	CO(1)+CO(2)+.468eV		2.76(-9)	2.86(-9)	
	CO(2)+CO(2)+.468eV	→	CO(2)+CO(2)+.468eV		3.72(-3)	3.93(-3)	
††	CO(0)+CO(1)+.734eV	→	CO(1)+CO(0)+.734eV		———	2.05(-3)	
	CO(0)+CO(2)+.468eV	→	CO(1)+CO(1)+.468eV		———	3.84(-5)	
	CO(0)+CO(2)+.468eV	→	CO(0)+CO(1)+.734eV		1.66(-8)	4.48(-7)	

* Figure in brackets indicates power of ten by which value to be multiplied.

** This process dominates the vibrational relaxation of CO. Evidently the two cross sections should be identical. Difference indicates the effect of 2 state coupling for A as against 3 state coupling for B.

† These cross sections properly identical with the previous V-T results. i.e.: structure in A neglected.

†† Exact resonance V-V processes.

IV. Laser Experiments

In this section we outline the progress made in the laser experiments over the past year. Our effort has been aimed at providing details of the gain profiles and vibrational distributions present in CW and pulsed CO laser systems for use in conjunction with modeling studies to completely elucidate the phenomenology operative in these laser systems.

The master laser oscillator was put into operation during the summer of 1972. Basically the system was composed of an 8 mm diameter discharge water cooled tube. The discharge was run from the ends of the tube to the center. An enhanced metal coated stainless steel mirror was used at one end and a grating wavelength selector in Littrow configuration was used as the reflector at the other end. Difficulties were encountered in room temperature operation. A variety of conditions was tried copying most of the published data but no output was measured. The tube was then cooled to dry ice temperature and CW lasing was monitored on more than forty CO spectral transitions. Powers ranged from microwatts to tens of milliwatts.

A small amount of ripple is present in our DC power supply. This results in large (up to 50%) intensity fluctuations in the laser output. An attempt made to filter this using an RC filter configuration was partially successful but it was felt higher stability was required. A current regulator was constructed after the design of Posakony (17) and this limited the output fluctuations to no more than a few percent. The probe oscillator was then ready for operation.

The test discharge cavity is not year operational due to difficulties with the suppliers of the gas monitoring equipment. In the meantime while awaiting supply, it was decided to attempt to understand why room temperature operation could not be achieved. Conditions in the discharge tube were monitored via end view spontaneous emission measurements under a variety of operating conditions. Analysis of this data is proceeding from two directions. In one effort artificial spectra are being generated in an attempt to match the observed spectra. In the other method a least squares fitting program has been written which combines gradient search techniques with an analytic solution developed from linearizing the fitting function. This method has been outlined by Bevington(18), and follows the technique of Marquardt(19). The program is operational and when tested on an artificially generated spectrum it obtained the vibrational temperature to within 0.7% in a time of about 3 seconds.

Figure 9 displays the intensity versus wavelength output from the grating selected master oscillator system at dry ice temperature. As noted by Bhaumik, et. al.(20), upon the addition of Hg vapor, the spectral output shifts as shown in Figure 10. The details associated with this shift, and possible shifts induced by the presence of other gas additives, may be very important in optimizing CO laser output. Experimental as well as analytical efforts are currently aimed at understanding this enhanced laser output.

A typical spontaneous emission endview measurement is shown in Figure 11 for dry ice conditions. Preliminary interpretation of the spectra shows that the rotational temperature is considerably higher than the wall temperature which undoubtedly is the reason that no lasing is observed under room temperature operation.

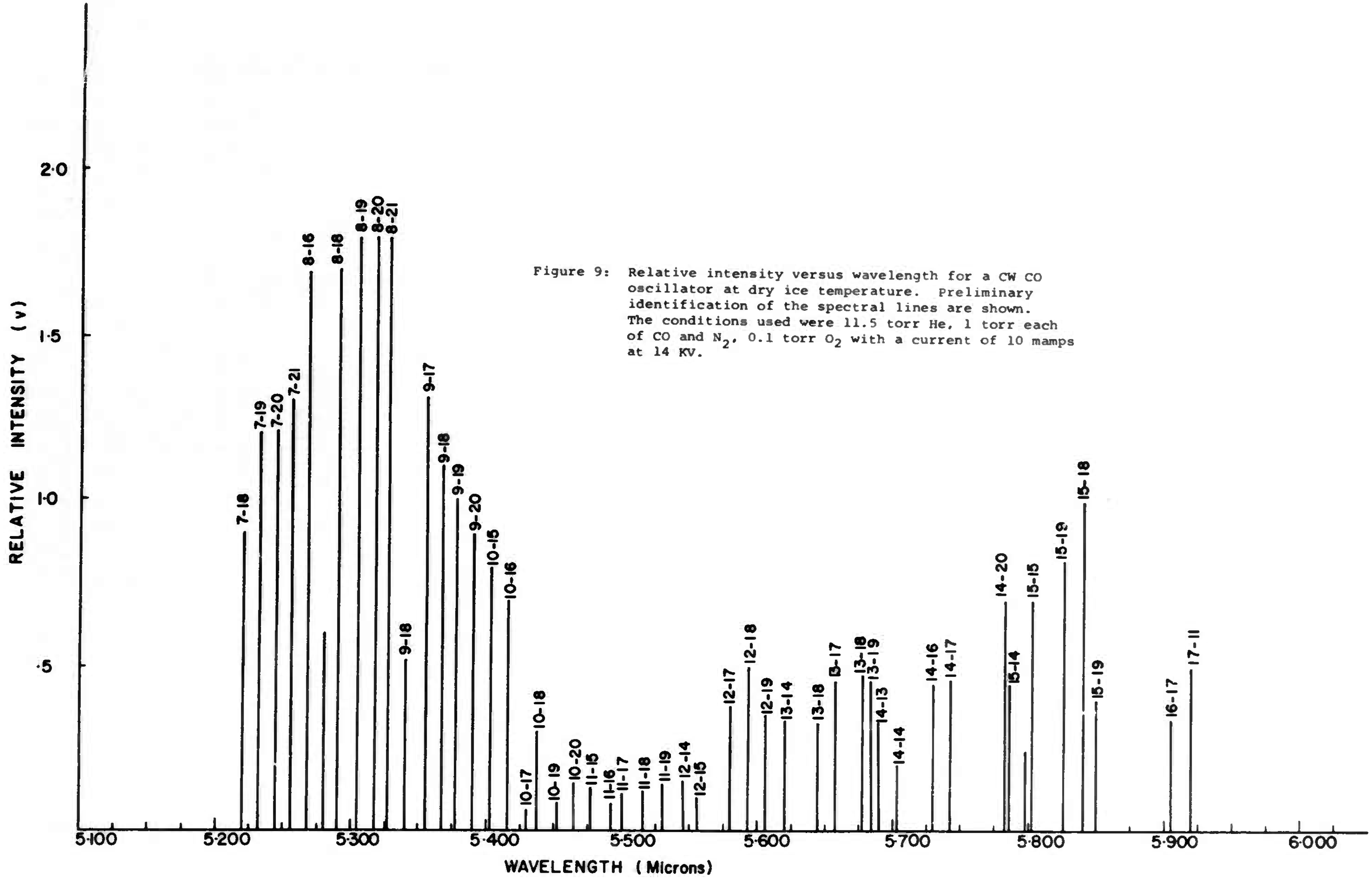

Figure 9: Relative intensity versus wavelength for a CW CO oscillator at dry ice temperature. Preliminary identification of the spectral lines are shown. The conditions used were 11.5 torr He, 1 torr each of CO and N_2, 0.1 torr O_2 with a current of 10 mamps at 14 KV.

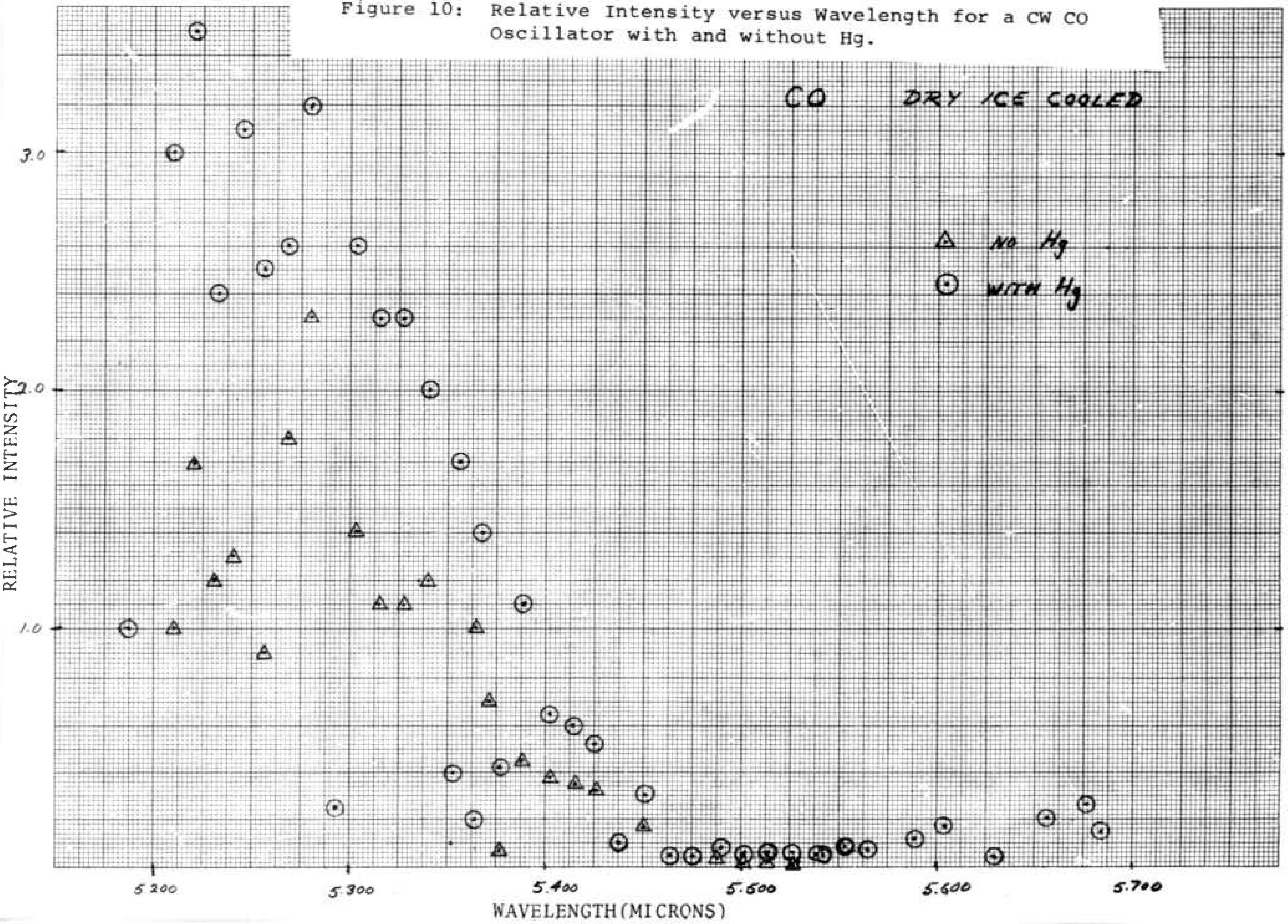

Figure 10: Relative Intensity versus Wavelength for a CW CO Oscillator with and without Hg.

Figure 11: Endview 1st Overtone Spectra from a CW CO Laser at room temperature. The Laser conditions were 1 torr CO, 2 torr N_2, 11.5 torr He, 5 mamps current and 500 µ slits.

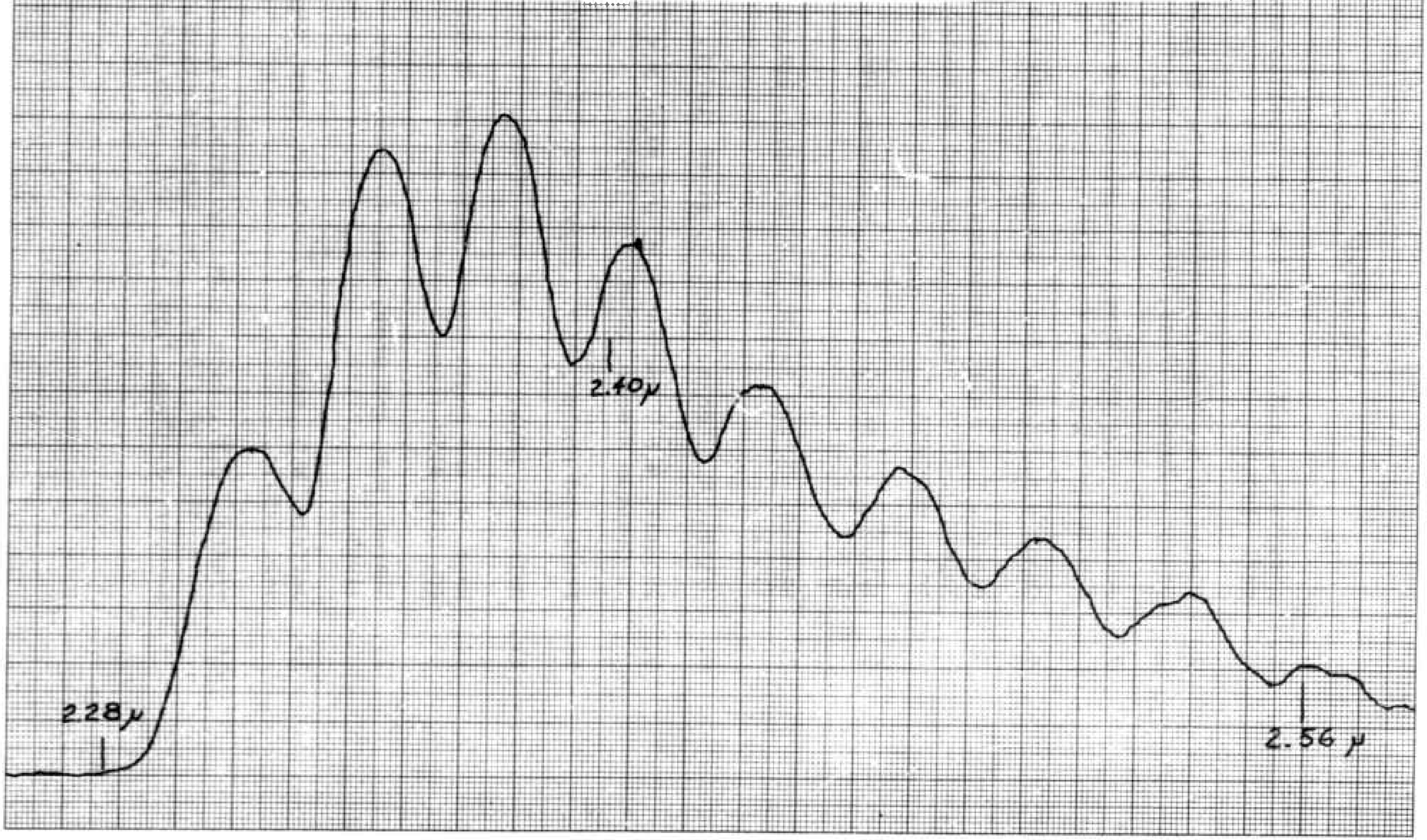

Bibliography

1. Abraham, G. and Fisher, E.R., J. Applied Phys. 43, 4621 (1972).

2. Fisher, E.R., Research Institute for Engineering Sciences Report 72-48, November (1972).

3. Jeffers, W.Q. and Wiswall, C.E., IEEE J. Quantum Electronics QE-7, 407 (1971).

4. Cohn, D.B., Appl. Phys. Letters 21, 343 (1972).

5. Fisher, E.R., A.F. Cambridge Research Labs Special Report 72-0539, August (1972) and references herein to R. Marriott.

6. Hancock, G. and Smith, I.W.M., Chem. Phys. Letters, 8, 41 (1971).

7. Hancock, G. and Smith, I.W.M., Appl. Optics 8, 1827 (1971).

8. Nighan, W.L. Phys. Rev., 2, A1989 (1970).

9. Bhaumik, M.L., Lacina, W.B. and Mann, M.M., IEEE J. Quantum Electr. QE-8, 150 (1972).

10. Frost and Phelps, A.V., Phys. Rev. 127, 1621 (1962).

11. Holstein, Phys. Rev. 70, 367 (1946).

12. Rapp, D. and Englander - Golden, P.J. Chem. Phys., 40, 573, 3120 (1964).

13. Sharma, R.D. and Brau, C.A. J. Chem. Phys. 50, 924 (1969).

14. Jeffers, W.Q. and Kelley, J.D., J. Chem. Phys. 55, 4433 (1971).

15. Treanor, C.E., Rich, J.W. and Rehm, R.G., J. Chem. Phys. 48, 1798 (1968). See also Fisher, E.R. and Kummler, J. Chem. Phys. 49, 1075, 1085 (1968).

16. Slawsky, A., Schwartz, R.N. and Herzfeld, K.F., J. Chem. Phys. 20, 10, 1591 (1952).

17. Posakony, M.J. Rev. Sci. Instr. 43, 270 (1972).

18. Bevington, R.P., Data Reduction and Error Analysis for the Physical Sciences, McGraw Hill (1969).

19. Marquardt, D.W., J. Soc. Ind. Appl. Math., 11, 431 (1963).

20. Mann, M.M., Bhaumik, M.L. and Lacina, W.B., Appl. Phys. Letters 16, 430 (1970).